JOURNAL GEOLOGICAL SOCIETY OF INDIA
Vol.72, August 2008, pp.263-277

Mineralogy and Geochemistry of the Bengal Anorthosite Massif in the Chotanagpur Gneissic Complex at the Eastern Indian Shield Margin

NARESH C. GHOSE[1]*, NILANJAN CHATTERJEE[2], DIPANKAR MUKHERJEE[3], RAY W. KENT[4] and A. D. SAUNDERS[5]

[1]Department of Geology, Patna University, Patna - 800 005, India
* G/608, Raheja Residency, Koramangala, Bangalore-560034
[2]Department of Earth, Atmospheric and Planetary Sciences, Massachusetts Institute of Technology, Cambridge, Massachusetts 02139, U.S.A.
[3]Geological Survey of India, Kankarbag, Patna - 800 020, India
[4]Research Office, Rutland Hall, Loughborough University, Loughborough, Leicester LE1 3TU.
[5]Department of Geology, Leicester University, Leicester LE1 7RH, U.K.
Email: ghosencprof@rediffmail.com

Abstract: The Bengal anorthosite is a narrow 40 km long, "tadpole-shaped" massif that occurs within granulite facies rocks of the Proterozoic Chotanagpur Gneissic Complex at the eastern margin of the Indian shield. The core of the massif consists of grey anorthosite with coarse-grained cumulus plagioclase megacrysts showing magmatic flow-related alignment and the periphery consists of a mixture of the megacrysts and medium-grained, equigranular white anorthosite. Repetitive graded layers of grey and white anorthosite and cyclic variation of elemental concentrations characterize the massif at depths. These features are consistent with emplacement of the Bengal anorthosite through episodic magma pulses. Labradorite (An_{57-58}) is the major constituent with clinopyroxene (Mg# 62), hornblende (Mg# 36-44), ilmenite and occasional orthopyroxene occurring as minor phases. Thermobarometric pressure-temperature estimates of the anorthosites (4.1-7.3 kbar and 593-795^{o}C) are similar to earlier studies achieved from the metabasic and gneissic country rocks, and correspond with the last high-grade (Grenvillian) metamorphism. Similar Zr/Nb, Zr/Hf and Th/Ce ratios of the anorthosites and oceanic island basalt possibly indicates derivation from a mantle source. Lower crustal interaction is evident from similar Zr/Y, La/Nb and Th/Ce ratios of the anorthosites and lower continental crust. Anatectic upper crustal melts probably contaminated the anorthosites as indicated from an enriched LILE pattern of the anorthosite. Metabasic rocks associated with the anorthosites have lower crustal Zr/Y, Nb/Y and Zr/Nb ratios. Minor gabbroic anorthosites within the massif, rich in iron and incompatible elements, were perhaps derived by differentiation of a coeval mafic parental magma. Proximity of the anorthosite to the Damodar Graben indicates that the Bengal anorthosite may have been emplaced in an extensional tectonic setting.

Keywords: Bengal anorthosite, Chotanagpur Gneissic Complex, Labradorite, Cyclic layers, Damodar Graben.

INTRODUCTION

Labradorite and/or andesine-rich Proterozoic anorthosite massifs have been recognized and investigated in many parts of the world (Ashwal, 1993; Wiebe, 1994). Remarkably, most of them were emplaced between 1.0 and 1.8 Ga in a variety of low to high metamorphic grade continental terrains. In spite of a voluminous literature on massif-type anorthosites, the cause and mechanism of their emplacement remains unsolved. Although high-pressure phase equilibrium indicates a lower crustal origin (Green, 1969; Taylor et al. 1984; Longhi et al. 1999; Longhi, 2005), it does not account for the large volume of magma required to generate the large plutons. Many researchers prefer a mantle plume-related origin and propose diapiric ascent of plagioclase-rich crystal-mush derived by extensive crystallization of the parental melts below the lower crust (Emslie, 1985; Ashwal, 1993). Isotopic evidence suggests that crustal contamination of the parental melts is rather common (Emslie et al.1994; Wiebe,1994). Some field evidence in the Nain plutonic suite suggests that the ascent

of the crystal-mush was aided by pre-existing faults and fractures (Royse and Park, 2000). Metamorphism is common in many massifs, but some massifs are undeformed (Emslie, 1978).

Proterozoic anorthosite massifs occur at the eastern margin of the Indian shield in two mobile belts (Fig. 1A), the Eastern Ghats Belt (EGB, Sarkar et al. 1981) and the Chotanagpur Gneissic Complex (CGC, Mukherjee and Ghose, 1992), where they are closely associated with high-grade amphibolite-granulite facies metamorphic rocks, sodic alkaline complexes and granite plutons. The Bengal anorthosite (Chatterjee, 1959) is an E-W elongated, "tadpole-shaped", 250 km^2 large massif at the eastern margin of the CGC. It is located between 23°27'48"N and 23°35'N latitudes and between 86°50'53"E and 87°15'E longitudes at Saltora, West Bengal (Fig. 1). Based on new mineralogical and geochemical data, the metamorphic history, geochemical character, probable source and emplacement mechanism of the Bengal anorthosite is evaluated in this paper.

Table 1. Stratigraphic relationships of the Bengal anorthosite and associated rocks

Age	Lithology
Recent	Alluvium
Early Tertiary	Salma dyke (dolerite)*
Permo-Carboniferous (Lower Gondwana)	Sandstone with shale partings and coal seams with intrusive dolerite, lamproite and lamprophyric rocks
----------	Unconformity ----------
	Pegmatite, aplite and quartz vein
	Alkali granite (hypersolvus)
	Biotite granite
Mesoproterozoic (1600-1400 Ma)	Syenite and nepheline syenite**
	Bengal Anorthosite massif***
	Basic granulite, amphibolite and hornblendite
Paleoproterozoic (>1600 Ma)	Supracrustal enclaves of metapelite (mica schist, sillimanite schists and khondalite), meta-arenite (quartzite and quartz-magnetite rock) and calc-silicate gneiss in basement complex comprised of quartzofeldspathic gneiss, migmatite, augen gneiss, biotite/ hornblende gneiss, charnockite, and leptynite

* 65.4 ± 0.3 Ma, Ar-Ar plateau age, Kent et al. (2002)
** 1475 ± 63 Ma, whole rock Rb-Sr isochron age, Ray Barman et al. (1994)
*** 1550 ± 2 Ma, U-Pb zircon age by ID-TIMS, Chatterjee et al. (2007)

GEOLOGICAL SETTING

The CGC is primarily composed of high-grade amphibolite-granulite facies basement gneisses and migmatite with enclaves of supracrustal metasediments intruded by mafic-ultramafic, massif anorthosite and granitic rocks (Ghose et al.1973; Ghose, 1983, 1992; Ghose and Mukherjee, 2000). The basement rocks exhibit polyphase deformation, metamorphism and partial melting, and record tectono-thermal events at 1.7-1.6 Ga and 0.9-1.1 Ga (Mallik et al. 1991; Ray Barman and Bishui, 1994; Singh et al. 2001; Maji et al. 2007). An older pre-1.6 Ga fabric is evident in sillimanite-bearing clasts of basal conglomerate (Ghose and Mukherjee, 2000) in the Bihar Mica Belt (Fig. 1B), a metamorphosed cover sequence in northern CGC intruded by granite at 1590 ± 30 Ma (Pandey et al. 1986). The Bengal anorthosite was emplaced at 1550 ± 2 Ma (U-Pb zircon age, Chatterjee et al. 2007). Younger magmatic events include Rajmahal basaltic volcanism at 115-118 Ma (Baksi, 1995; Kent et al. 2002) and Salma mafic dyke intrusion at 65.4 ± 0.3 Ma (Kent et al. 2002) (Fig.1C). Based on available geochronological data and mutual relationship of rocks, a simplified stratigraphic sequence of the eastern part of the CGC is presented in Table 1.

In the vicinity of the Bengal anorthosite (Fig. 1), the basement rocks include quartzofeldspathic gneiss, biotite (bt)-hornblende (hbl) gneiss, hbl gneiss, migmatite, charnockite and leptynite, and the supracrustal meta-sediments include calc-silicate granulite, quartzite, mica schist, khondalite, sillimanite schist and quartz (qtz)-magnetite (mag) rock. The anorthosite and subsequently granites intruded the granulite to amphibolite facies country gneisses and metasediments. Several bands of metabasic rocks (mafic granulite and amphibolite) containing plagioclase (pl), hbl, clinopyroxene (cpx)±orthopyroxene (opx)±garnet (grt) occur both inside and outside the massif (Ghose et al. 2005). They are parallel to the E-W regional trend (Fig. 1C) and show branching and pinch-and-swell structures inside the massif. Folded veins and tongues of anorthosite occur within the metabasic rocks (Mukherjee, 1995) and metabasic xenoliths occur within the anorthosite (Fig. 2A) indicating that the anorthosite and metabasic suites are coeval. Previous thermobarometric calculations indicated similar pressures and temperatures (P-T) for the Bengal anorthosite, metabasites and the country rocks (4.0-8.5 kbar/600-830°C, Table 2, Fig. 3). Sen and Bhattacharya (1993) interpreted ~7.5 kbar and ~830°C as conditions slightly below that of peak metamorphism. Recent work has attempted to correlate P-T's (Maji et al. 2007) to metamorphism associated with the three recognizable deformations (D_1, D_2 and D_3) in the area (Roy, 1977; Mukherjee, 1995).

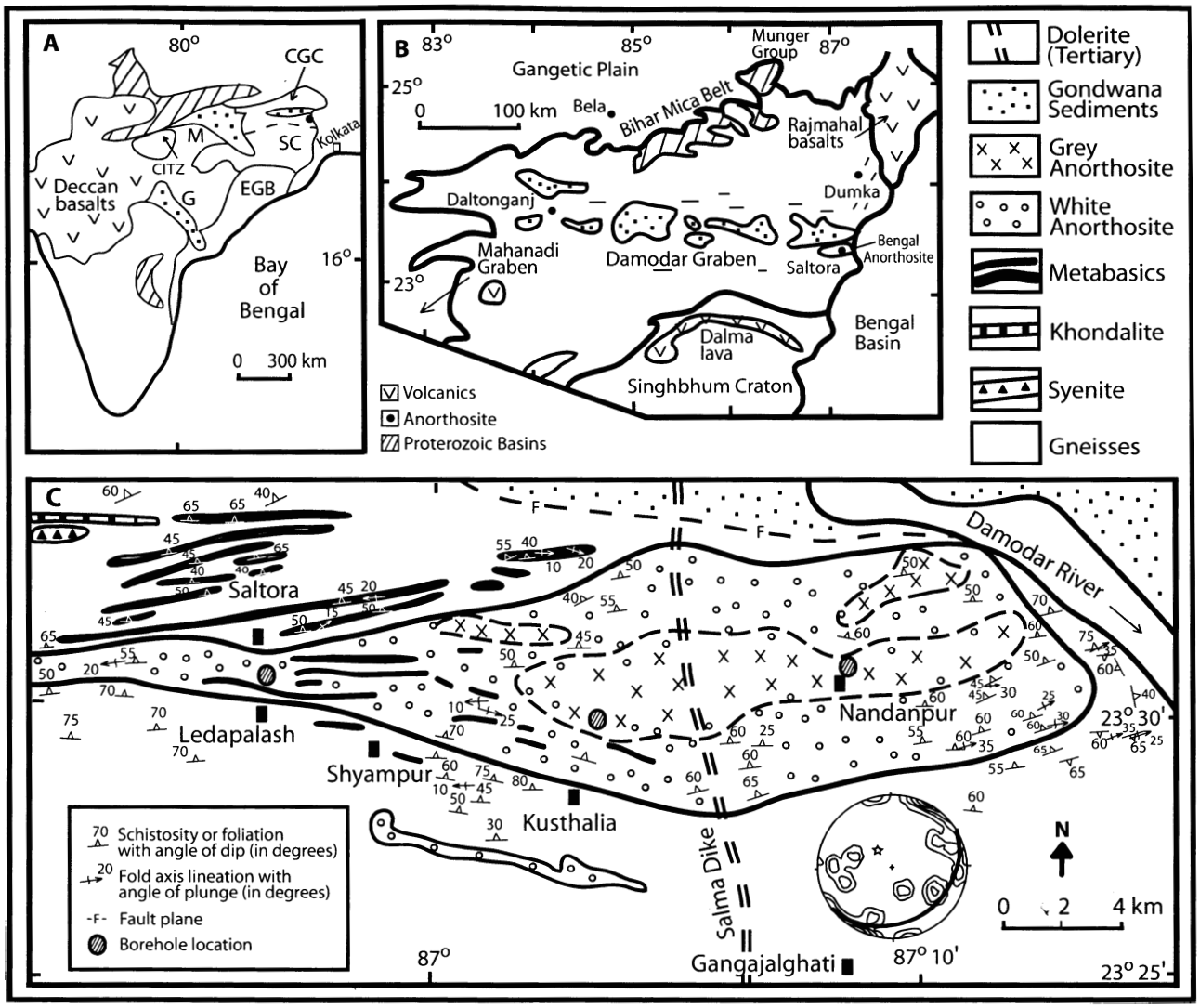

Fig.1. (A) Location map of the Bengal anorthosite at Saltora (solid circle), Eastern India. EGB - Eastern Ghats Belt, SC - Singhbhum craton, CGC - Chotanagpur Gneissic Complex, CITZ - Central Indian Tectonic Zone, dashed line - Singhbhum shear zone, stippled area - Gondwana Basins: M-Mahanadi Basin, G-Godavari Basin. **(B)** A simplified map of the CGC showing location of the Bengal anorthosite at Saltora and other anorthosite occurrences (solid circle), Gondwana Basins along the Damodar Graben (stippled area) and Proterozoic Basins (inclined bars). **(C)** A detailed map of the Bengal anorthosite and its surrounding areas (modified after Roy, 1977; Bhattacharyya and Mukherjee, 1987) and an orientation plot for primary flow structures in anorthosite (*after* Mukherjee, 1995).

In and around Saltora, the poorly preserved earliest non-diastrophic sedimentary stratification (S_0) was deformed during D_1 to tightly appressed, isoclinal, rootless, intrafolial folds with E-W northerly-dipping axial planes (S_1). The S_1 fabric is characterized by inclusions of pl+ilmenite (ilm)±hbl in opx and cpx in mafic granulites, grt+opx in pl-bearing leucocratic and bt±hbl melanocratic layers in migmatitic gneisses, cpx+scapolite (scp)+pl+K-feldspar (kfs)+calcite (cc)+qtz in calc-silicate gneisses, and grt+sillimanite (sil)+kfs+qtz+spinel (spl)+ilm in metapelites (Maji et al. 2007). These authors further suggest that inclusions of bt, pl, kfs and ilm in gt indicate a prograde formation of garnet accompanied by melting at 750–850ºC and 4-6 kbar. The Bengal anorthosite lacks the S_1 granulitic fabric, but contains the subsequent fabrics. Hence, it is post-D_1/pre-D_2 and was emplaced into D_1-deformed high-grade gneisses (Maji et al. 2007) at 1.55 Ga (Chatterjee et al. 2007).

The D_2 episode produced asymmetric and overturned folds coaxial with the first generation folds. S_1 was isoclinally folded during D_2 with development of a

Table 2. Equilibrium pressures and temperatures of the anorthosites and associated rocks

	T°C (min)[a]	T°C (max)[a]	P kbar (min)[a]	P kbar (max)[a]	Equilibria	Formulation[b]	Reference[c]
				Massif			
Amphibolite/Meta-norite	761	807	*5*		hbl-plag	15	C
Amphibolite/Meta-norite	619	670	*6*		two-px	18	C
Basic granulite	768	794	*6.3*		two-px	16	A
Basic granulite	619	665	*6.3*		opx-gar	14	A
Basic granulite	604	659	*6.3*		cpx-gar	7	A
Basic granulite	711	761	*6.3*		cpx-gar	9	A
Basic granulite	*650*	*750*	5.7	6.6	px-gar-plag-qtz	21	A
Amphibolite/Meta-norite	*761*	*807*	6.4		*hbl-plag*, Al-in-hbl	*15*, 1	C
Gabbroic anorthosite	704	736	*5*		hbl-plag	15	C
Gabbroic anorthosite	729	757	*5*		hbl-plag	15	C
Gabbroic anorthosite	625	658	*6*		two-px	18	H
Gabbroic anorthosite	623				gar-bt	8	H
Gabbroic anorthosite	641				gar-hbl	12	H
Gabbroic anorthosite[d]	616	672	4.3	4.7	cpx-gar, cpx-gar-plag-qtz	7, 21	H
Gabbroic anorthosite[d]	593	649	4.3	4.7	cpx-gar, cpx-gar-plag-qtz	24, 21	H
Gabbroic anorthosite	616	672	4.1	4.4	cpx-gar, cpx-gar-plag-qtz	7, 21, 6	H
Gabbroic anorthosite	*704*	*736*	5.6	6.1	*hbl-plag*, Al-in-hbl	*15*, 1	C
White anorthosite	669		*5*		hbl-plag	15	H
Mottled anorthosite	726	795	*5*		hbl-plag	15	H
Anorthosite	720		*7*		opx-gar	25	E
Anorthosite	670		*7*		opx-gar	14	E
Anorthosite	645	715	*6*		opx-gar/cpx-gar	14, 25, 7	E
White anorthosite	724				gar-bt	8	H
White anorthosite	646				gar-hbl	12	H
Anorthosite	*600*	*800*	6.6	7.4	opx-gar-plag-qtz	21	E
White anorthosite	*683*	*696*	5.6	7.3	*hbl-plag*, Al-in-hbl	*15*, 1	H
				Country Rocks			
Meta-norite	778	800	*5*		hbl-plag	15	C
Amphibolite	667	724	*5*		hbl-plag	15	H, B
Meta-norite	638	659	*6*		two-px	18	C
Basic granulite	620	720	*7*		opx-gar	25	G
Basic granulite	600	630	*6*		opx-gar	14, 3	F
Basic granulite	660	700	*6*		opx-gar	25	F
Basic granulite	720	740	*6*		opx-gar	17, 3	F
Basic granulite	650	720	*7*		cpx-gar	7	G
Basic granulite	650	700	*6*		cpx-gar	7, 3	F
Basic granulite	*650*	*690*	6.6	7.4	Fe-opx-gar-plag-qtz	22	F
Basic granulite	*650*	*690*	6.5	7.5	Fe-opx-gar-plag-qtz	19	F
Basic granulite	*650*	*690*	5.7	7.1	Fe-cpx-gar-plag-qtz	19	F
Khondalite	742		*6.3*		cpx-gar	9	A
Metapelite	645	715	*6*		opx-gar/cpx-gar	14, 25, 7	E
Metapelite	630	700	*7*		gar-bt	8	E
Khondalite	*650*	*750*	5.9	6.5	gar-plag-qtz-sill	20	A
Metapelite	*600*	*800*	4	5.4	gar-plag-qtz-sill	10, 20	E
Basic granulite	750	830	6	8.5	hbl-px-plag-gar	4, 13, 5	D
Calc-silicate gneiss	820	840	7.3	7.6	plag-calc-scap-gar	11, 23, 2	F

[a] Italicized T and P values are assumed values

[b] These references are available from the authors upon request: 1 - Anderson and Smith (1995), 2 - Berman (1988), 3 - Bhattacharya et al. (1990), 4 - Binns (1969), 5 - Brown (1970), 6 - Eckert et al. (1991), 7 - Ellis and Green (1979), 8 - Ferry and Spear (1978), 9 - Ganguly (1979), 10 - Ganguly and Saxena (1984), 11 - Goldsmith and Newton (1977), 12 - Graham and Powell (1984), 13 - Green and Ringwood (1967), 14 - Harley (1984), 15 - Holland and Blundy (1994), 16 - Kretz (1982), 17 - Lee and Ganguly (1988), 18 - Lindsley (1983), 19 - Moecher et al. (1988), 20 - Newton and Haselton (1981), 21 - Newton and Perkins (1982), 22 – Perkins and Chipera (1985), 23 - Powell (1978), 24 - Powell (1985), 25 - Sen and Bhattacharya (1984)

[c] A - Bhattacharyya and Mukherjee (1987), B - Das and Bhattacharyya (1999), C - Ghose et al. (2005), D - Manna and Sen (1974), E - Sen and Bhattacharya (1985), F - Sen and Bhattacharya (1993), G - Sen and Manna (1976), H - This study

[d] calculated from cores (higher P,T) and rims (lower P,T) of the coexisting minerals

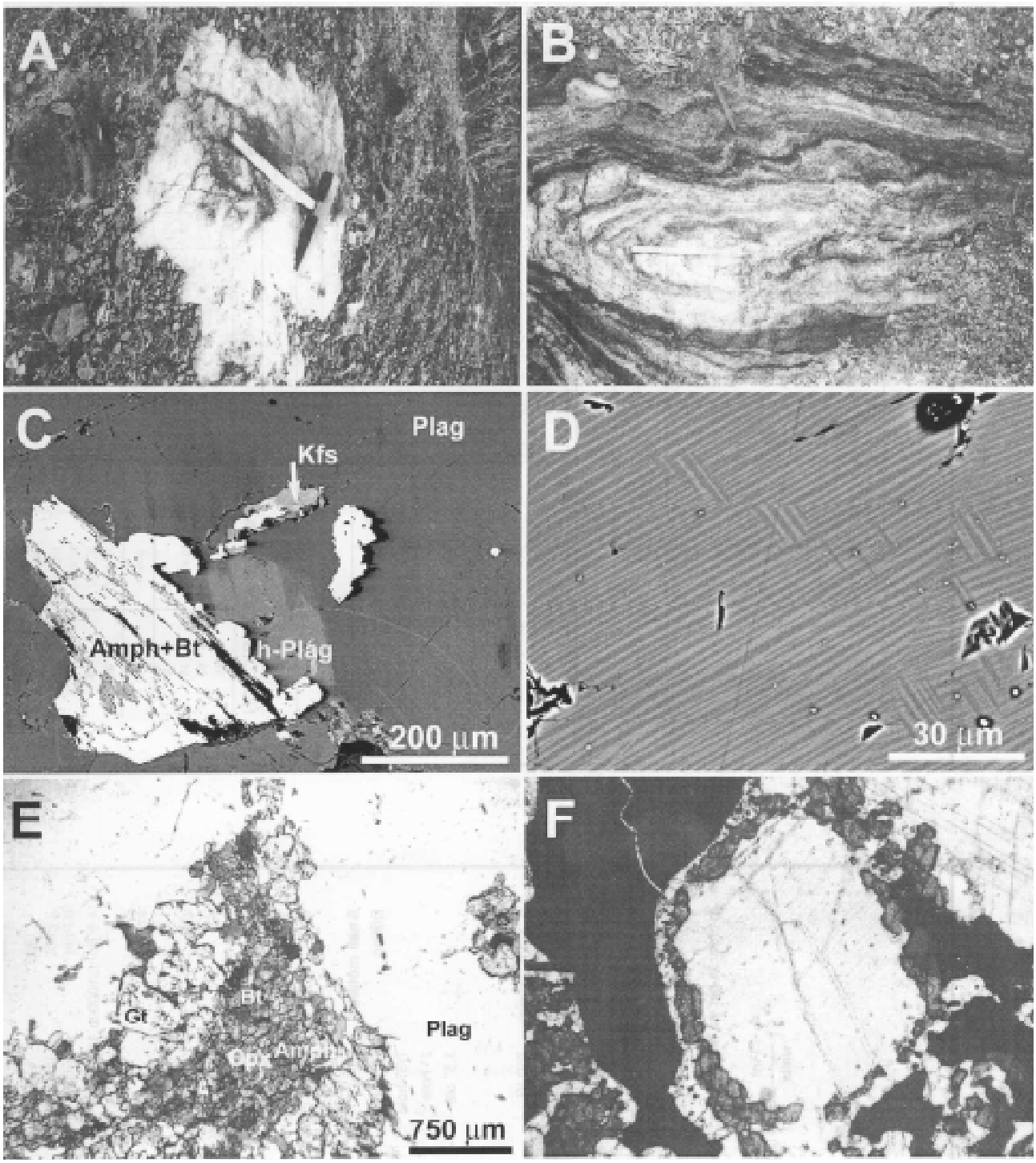

Fig.2. (**A**) Metabasic xenolith within anorthosite north of Nandanpur showing diffuse contact, the hammer is placed on the metabasic. (**B**) Superposition of upright F_3 fold (axial trace upward in photo) on the limb of isoclinal F_2 fold (axial trace side-to-side in photo, see pencil for scale) of basement gneiss, xenolith within anorthosite south of Sitaldanga. (**C**) Back-scattered electron image showing plagioclase with huttenlocher intergrowth (h-Plag) growing between amphibole (Amph) + biotite (Bt) and K-feldspar (Kfs). (**D**) Details of the huttenlocher intergrowth in plagioclase. (E) Crossed polarized light image showing garnet (Gt) corona around clinopyroxene (Cpx), amphibole and biotite surrounded by plagioclase. (F) Plane light image showing garnet corona around plagioclase (width ~2 mm) with an outer rim of Fe-Ti oxide in white anorthosite from a borehole sample at Nandanpur.

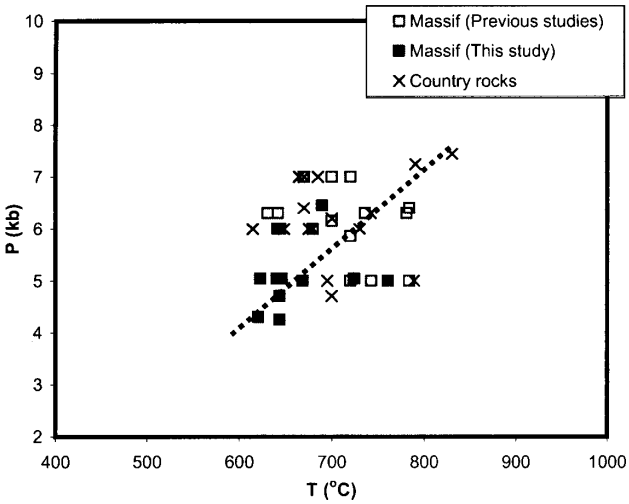

Fig.3. Calculated equilibrium pressures and temperatures of anorthosite, amphibolite, basic granulite, metapelite and calc-granulite from the Bengal anorthosite massif and the surrounding country rocks. The arrow indicates an approximate retrograde metamorphic pressure-temperature trajectory. Data include earlier works of Bhattacharyya and Mukherjee (1987), Ghose et al. (2005), Manna and Sen (1974), Sen and Bhattacharya (1985, 1993) and Sen and Manna (1976) (*see* Table 2) for comparison.

penetrative foliation (S_2) defined by the preferred alignment of hbl in mafic granulite, bt in quartzofeldspathic gneisses, and bt+sil aggregates in metapelites (Mukherjee, 1995; Maji et al. 2007). D_3 resulted in a set of east-west north-dipping asymmetric, upright non-cylindrical shear related folds (Fig. 2B). The expansive granites were deformed during D_3 under upper amphibolite facies conditions at 1.4 -1.1 Ga (Maji et al. 2007). The S_2 and S_3 fabrics are characterized by bt±sil in gneiss and metapelite that formed at the expense of grt, and hbl in mafic granulite that formed at the expense of opx+cpx+pl. In the anorthosite massif, S_2 and S_3 consist of hbl+pl and shape-preferred bt. The intensity of deformation decreases inward in the massif. In the interior part, deformation is limited to weak wavy extinction, mildly bent twin lamellae and local bulges at grain boundaries in plagioclase. In the peripheral parts, internally strained plagioclase forms a fine-grained mosaic including coarse-grained elliptical plagioclase of magmatic origin with sub-grain boundaries.

Post-D_3 Grenvillian metamorphism at 0.9-1.0 Ga (Maji et al. 2007; Chatterjee et al. 2007) was marked by prograde growth of coronal and discrete grt (+qtz) at opx-pl interface in mafic granulite and gneiss at the expense of bt+pl, and opx-pl and hbl-pl interfaces in anorthosite at the expense of opx and cpx at 650 ± 50ºC and 4.5 ± 0.5 kbar.

The core of the Bengal anorthosite is composed of grey anorthosite (colour index ‹8) containing coarse-grained, bluish grey cumulus plagioclase megacrysts showing magmatic flow-related alignment (Mukherjee et al. 2005). Anorthosite dykes also showing magmatic alignment of euhedral plagioclase occur near the core of the massif (Maji et al. 2007). The plagioclase megacrysts are poikilitic with small inclusions of ilm, mag and bt. The periphery of the massif is dominated by medium grained, equigranular white anorthosite (colour index =8). The texture gradually changes from panidiomorphic at the core to saccharoidal near the periphery as the proportion of white granular plagioclase increases. The zone between the grey and the white anorthosites has a mottled appearance due to variable amounts of the grey and white plagioclase. Schlierens of opx-cpx-hbl-grt-bt-ilm give the anorthosites a banded appearance. A few isolated pods of grey anorthosite occur within the mottled anorthosite in the northern part of the massif (Fig. 1C) and a small pocket of gabbroic anorthosite occurs within the mottled anorthosite northeast of Ledapalash. Lenses and bands of ilm, mag and spl-rich rocks occur at the northern boundary of the massif (Bose and Roy, 1966).

The sub-surface shape of the Bengal anorthosite is sheet-like (Chatterjee, 1959) or an inverted cone/wedge as inferred from gravity data (Verma et al. 1975; Mukhopadhyay, 1987). Deep drilling up to a depth of 622.8 m from the surface at three locations within the massif (Fig. 1C; Mukherjee, 1995; Mukherjee et al. 2005) revealed repetitive graded layers of grey, white and mottled anorthosites overlain by gabbroic anorthosite. The basal part of the anorthosite pluton is essentially composed of denser equigranular white anorthosite as revealed from the borehole sections. Plagioclase megacrysts and mafic schlierens show flow-related preferred orientation, and grt coexists with opx, cpx, hbl, mag and ilm throughout the boreholes. Muscovite, bt, chlorite, cc, scp and epidote are present in the upper and the peripheral parts of the massif. Pockets of syenite, alkali granite, pegmatite and aplite, and veins of quartz and calcite are also encountered in the boreholes.

ANALYTICAL METHODS

Textures were studied with a polarizing light optical microscope and by backscattered electron imaging with a JEOL JXA-733 Superprobe at Massachusetts Institute of Technology, Cambridge, U.S.A. Major element composition of minerals were analyzed by wavelength dispersive spectrometry with the same electron microprobe. The accelerating voltage and beam current used were 15 kV and 10 nA, respectively. Typical counting times were 20-40

seconds and 1σ standard deviations of the counts were 0.5-1%. The data were reduced with the CITZAF program (Armstrong, 1995). The mineral analysis data are presented in Table 3.

Samples of anorthosite and associated rocks were analyzed for major and trace element concentrations with wavelength-dispersive X-ray fluorescence spectrometry (WD-XRF) at the Department of Geology, Leicester University, U.K. Samples were crushed with a tungsten-carbide crusher, powdered in an agate mortar and pressed into pellets. Several international geostandards for major (MRG-1, W-1 and GA) and trace (MRG-1, W-1, W-2 and BR) elements were analyzed simultaneously for internal consistency and to monitor the precision of the analytical data. FeO was determined by titration following digestion of sample in a mixture of analytical grade HF and concentrated H_2SO_4 in a platinum crucible on hot plate. The chemical analyses of samples are presented in Table 4. The percentage average differences from the published values of the monitor standards (Govindaraju,1994) are 0.3-2% for major oxides, 3-13% for the minor oxides, 1-18% for the incompatible elements (including light rare earths) and 0.1-25% for the compatible trace elements. These differences are within the 2σ analytical uncertainties of the WD-XRF measurements. Four samples of anorthosite were also analyzed by neutron activation analysis (NAA) for rare-earth (REE) and some critical trace elements (Sc, Ta, Hf and Th) at the Geological Survey of India, Pune. These data are shown in Table 5.

PETROGRAPHY, MINERAL CHEMISTRY AND METAMORPHISM

The Bengal anorthosite is dominated by labradorite. A distribution diagram for 136 analyses of plagioclase, selected from six samples of grey, white and mottled anorthosites, shows a well-characterized peak between An_{57} and An_{58} (Table 3, Fig. 4). The grey plagioclase megacryst cores are An_{55-63} in composition. They show kink twin lamellae, micro-fracture, peripheral granulation and contain fine inclusions of ilmenite, iron oxide and biotite (Mukherjee et al. 2005). The white granular plagioclase with a wider range of composition (An_{51-66}) forms a polygonal mosaic with sharp boundaries and 120° "triple-point" contacts. Some show albite- or pericline-twin lamellae and kink bands. Both plagioclase-types show subtle compositional zoning. In some samples, small Ca-rich plagioclase (An_{69-80}) grains associated with hornblende, biotite and K-feldspar show huttenlocher intergrowths (Figs. 2C,D). Subordinate amounts (<8% by volume) of augite (Mg# 62) and hornblende (Mg# 36-44, CaO 11.1-11.5 wt %) are present in mafic clots and schlierens in the anorthosites (Table 3, Fig. 2E). Augite contains exsolved lamellae of ortho-pyroxene and blebs of ilmenite. Corona forming garnet (Figs. 2E,F) is almandine-rich ($Gr_{18}Pyr_{13}Alm_{65}$). Biotite (Mg# 43-46), K-feldspar and quartz occur in minor amounts and magnetite, pyrite, apatite, sphene and zircon occur as accessory minerals. Chlorite, muscovite, zoisite, epidote, actinolite, scapolite and calcite occur as secondary alteration products.

The gabbroic anorthosite contains 10-17% mafic minerals by volume. It consists of plagioclase (An_{43-52}), clinopyroxene (Mg# 59-64) and hornblende (Mg# 41-45) with minor amounts of orthopyroxene (Mg# 45-48), biotite (Mg# 36-42), garnet ($Gr_{22}Pyr_{12}Alm_{63}$), chlorite and ilmenite. The compositions of clinopyroxene, plagioclase, hornblende and orthopyroxene are similar to those of the metabasic rocks inside the anorthosite massif (Ghose et al. 2005). Accessory phases include apatite, zircon, K-feldspar, chlorite, epidote and magnetite.

Garnet corona around clinopyroxene and/or hornblende, and intergrowths of grt+ilm+hbl between plagioclase grains originated through high-grade metamorphism during the post-D_3 stage (Figs. 2E,F). Biotite, plagioclase, hornblende and K-feldspar may be related through chemical reaction (Fig. 2C). Huttenlocher intergrowths in the high-Ca plagioclase grains (An_{70-80}) (Fig. 2D) probably originated by slow cooling (Grove,1977). Rims of secondary actinolite (Mg# 60) around clinopyroxene (Mukherjee et al. 2005) may have formed later through hydrous alteration. A variety of mineral equilibria including two-pyroxene (Lindsley, 1983), grt-bt (Ferry and Spear, 1978), grt-hbl (Graham and Powell, 1984), cpx-grt-pl-qtz (Ellis and Green, 1979; Newton and Perkins, 1982) and hbl-pl (Holland and Blundy, 1994; Anderson and Smith, 1995) were used to calculate pressures of 4.1-7.3 kbar and temperatures of 593-795°C in the anorthosites. These results are similar to those for the country rocks and metabasic rocks inside and outside the massif (Bhattacharyya and Mukherjee, 1987; Ghose et al. 2005; Maji et al. 2007) and define a common pressure-temperature path for the massif and the surrounding rocks during post-D_3 Grenvillian metamorphism (Fig. 3).

GEOCHEMISTRY

Both the earlier published (Mukherjee et al. 2005) and the new data in this study (Table 4) indicate that the grey anorthosite is richer in Al_2O_3 and K_2O, and poorer in TiO_2, MgO, P_2O_5, Zr, light rare earth elements (LREE), Ba, Sr, Zn and the transition elements, viz. Fe, Mn, V, Cr and Ni

Table 3. Chemical composition of minerals in the Bengal anorthosite

Sample	Plagioclase											K-feldspar	
	C11		C19		C22		B30	B10		B36		C11	C19
	core	rim	megacryst	granular	granular	huttenlocher	megacryst	megacryst	granular	megacryst	granular		
No. of analyses	5	2	15	29	24	10	10	4	11	10	9	1	1
						weight percent							
SiO_2	56.07	56.70	53.74	53.06	53.44	49.52	53.16	53.30	53.69	53.00	53.41	64.18	64.13
Al_2O_3	28.39	28.06	30.21	30.40	30.00	32.79	30.04	30.07	29.73	30.41	30.18	19.32	19.53
FeO	0.16	0.27	0.04	0.04	0.08	0.07	0.09	0.11	0.07	0.09	0.10	0.28	0.04
MgO	bdl	0.02	0.01	0.01	0.01	bdl	0.01	bdl	bdl	bdl	bdl	0.01	bdl
CaO	10.09	9.54	11.93	12.12	11.89	15.12	11.94	11.90	11.70	12.37	12.10	0.05	0.08
Na_2O	5.75	6.13	4.67	4.49	4.68	2.92	4.62	4.84	4.94	4.46	4.52	0.70	0.57
K_2O	0.15	0.13	0.10	0.09	0.09	0.04	0.18	0.18	0.15	0.17	0.17	14.41	14.91
BaO			0.02	0.07	0.12							2.31	2.73
Total	**100.62**	**100.82**	**100.74**	**100.29**	**100.30**	**100.46**	**100.03**	**100.38**	**100.29**	**100.51**	**100.50**	**101.27**	**101.99**
						atoms							
Si	2.507	2.527	2.411	2.393	2.410	2.249	2.404	2.404	2.421	2.388	2.404	2.958	2.948
Al	1.496	1.474	1.597	1.616	1.595	1.755	1.601	1.598	1.580	1.615	1.601	1.050	1.058
Fe	0.006	0.010	0.002	0.002	0.003	0.003	0.003	0.004	0.003	0.003	0.004	0.011	0.001
Mg		0.001	0.001	0.001	0.001		0.001					0.001	
Ca	0.483	0.456	0.574	0.586	0.575	0.736	0.579	0.575	0.565	0.597	0.584	0.002	0.004
Na	0.499	0.529	0.406	0.393	0.409	0.258	0.405	0.423	0.432	0.390	0.395	0.063	0.051
K	0.008	0.007	0.006	0.005	0.005	0.002	0.010	0.010	0.009	0.010	0.010	0.847	0.874
Ba				0.001	0.002							0.042	0.049
O	8	8	8	8	8	8	8	8	8	8	8	8	8
ΣCation	4.999	5.004	4.997	4.998	5.000	5.003	5.003	5.014	5.010	5.004	4.998	4.973	4.986
Or[a]	0.9	0.7	0.6	0.5	0.5	0.2	1.0	1.0	0.9	1.0	1.0	88.8	89.3
An[a]	48.8	45.9	58.2	59.4	58.0	73.9	58.2	57.0	56.2	59.9	59.0	0.3	0.4
Ab[a]	50.3	53.4	41.2	39.9	41.3	25.9	40.7	42.0	42.9	39.1	39.9	6.6	5.2
Cs[a]				0.1	0.2							4.4	5.0

Sample	hornblende				actinolite	augite		opx	biotite			garnet		ilmenite	
	C11	C19	C22	B30 rims cpx	C11 rims cpx	C11	B30	C11	C11	C19	C22	C11	C22	C11	C22
No. of analyses	3	1	5	1	1	6	2	4	5	1	4	15	10	2	2
							weight percent								
SiO_2	41.84	41.29	42.29	38.72	53.43	51.68	52.28	50.28	35.79	36.08	35.08	37.85	37.58	0.00	0.00
TiO_2	1.92	1.37	1.19	3.29	0.16	0.11	0.15	0.04	4.22	3.38	3.91	0.06	0.03	51.54	51.79
Al_2O_3	12.22	13.73	13.30	13.87	2.28	1.31	1.47	0.79	15.53	16.83	15.57	21.95	22.00	0.03	0.08
Cr_2O_3	bdl	bdl	0.03	0.02	bdl	bdl	bdl	0.01	0.01	0.04	bdl	0.01	0.01	0.02	bdl
FeO	19.83	20.48	19.07	19.82	16.17	12.73	12.64	31.76	23.14	23.05	21.43	28.79	29.25	47.35	46.66
MnO	0.13	0.37	0.20	0.17	0.17	0.19	0.35	0.43	0.06	0.09	0.08	1.38	2.05	0.33	0.67
MgO	7.80	6.60	8.27	6.34	13.82	11.08	11.24	15.37	8.28	8.22	9.89	3.03	3.28	0.30	0.27
CaO	11.54	11.42	11.12	11.44	11.92	22.57	22.03	0.53	0.07	0.06	0.12	8.03	6.29	0.02	0.03
Na_2O	1.15	0.78	1.39	1.30	0.16	0.30	0.42		0.07	0.14	0.12	0.01	0.01		
K_2O	1.59	1.69	0.87	2.65	0.12				8.79	8.95	8.19				
NiO						0.02		0.02						bdl	0.05
F	0.01	0.02	bdl	bdl	bdl				0.08	0.13	0.04				
Cl	0.12	0.50	0.17	0.72	bdl				0.14	0.41	0.19				
Total	**98.16**	**98.25**	**97.90**	**98.34**	**98.23**	**99.98**	**100.57**	**99.21**	**96.19**	**97.38**	**94.62**	**101.11**	**100.48**	**99.57**	**99.56**
							atoms								
Si	6.367	6.301	6.385	5.980	7.758	1.967	1.973	1.979	5.501	5.718	5.435	2.969	2.968	0.000	0.000
Ti	0.220	0.157	0.136	0.382	0.018	0.003	0.004	0.001	0.488	0.403	0.456	0.004	0.002	0.986	0.989
Al	2.193	2.470	2.366	2.525	0.390	0.059	0.065	0.037	2.813	3.145	2.843	2.029	2.048	0.001	0.002
Cr			0.003	0.003				0.000	0.001	0.005		0.000	0.001	0.000	
Fe	2.524	2.614	2.408	2.560	1.964	0.405	0.399	1.045	2.974	3.055	2.777	1.889	1.932	1.007	0.991
Mn	0.017	0.047	0.025	0.022	0.021	0.006	0.011	0.014	0.007	0.012	0.011	0.091	0.137	0.007	0.014
Mg	1.771	1.501	1.862	1.458	2.991	0.629	0.632	0.902	1.896	1.942	2.285	0.354	0.386	0.011	0.010
Ca	1.881	1.867	1.799	1.893	1.854	0.920	0.891	0.022	0.012	0.010	0.020	0.675	0.532	0.000	0.001
Na	0.340	0.229	0.408	0.388	0.044	0.022	0.031	0.000	0.020	0.042	0.036	0.001	0.001		
K	0.308	0.329	0.168	0.523	0.023				1.724	1.810	1.618				
Ni						0.001		0.001							0.001
F	0.006	0.011							0.039	0.066	0.018				
Cl	0.030	0.130	0.044	0.189					0.038	0.111	0.051				
O	22.964	22.720	22.956	22.622	23	6	6	6	21.923	22.646	21.931	12	12	3	3
ΣCation	15.658	15.657	15.604	15.924	15.062	4.011	4.006	4.001	15.514	16.318	15.549	8.013	8.006	2.013	2.009
Mg#[c]	41.2	36.5	43.6	36.3	60.4	60.8	61.3	46.3	38.9	38.9	45.1	15.8	16.6		
En or Pyr[b]						32.2	32.9	45.8				11.8	12.9		
Fs or Alm[b]						20.7	20.8	53.1				62.8	64.7		
Wo or Gro[b]						47.1	46.3	1.1				22.4	17.8		
Spe[b]												3.0	4.6		

[a] Or - orthoclase, An - anorthite, Ab - albite, Cs - Celsian; [b] En - enstatite, Fs - ferrosilite, Wo - wollastonite, Pyr - pyrope, Alm - almandine, Gro - grossular, Spe - spessartine
[c] Mg# = 100[Mg/(Mg+Fe)]; bdl: below detection limit

Table 4. Chemical composition of the Bengal anorthosites

Sample[a]	gabbroic			grey		mottled				white					BenAn	Lti-meta	OIB	UCC	LCC
	B12	B30	avg(5)	B36	avg(3)	B10	B37	B8	avg(8)	B1	B23	C27	B21	avg(9)	avg(25)	avg(5)			
Location[b]	1	2		3		1	4	1		1	5	1	6						
weight percent																			
SiO_2	45.73	51.08	45.76	51.02	50.93	50.75	48.82		49.25	48.67	49.26		48.93	49.20	48.95	47.28			
TiO_2	3.49	0.11	2.52	0.19	0.24	0.15	0.13		0.98	0.16	1.21		0.49	0.65	0.98	1.55			
Al_2O_3	14.50	28.47	16.48	28.23	28.40	27.69	28.15		25.54	29.06	24.02		26.45	25.64	24.60	12.39			
Fe_2O_3	3.44	0.28	2.70	0.38	0.39	0.53	0.12		1.03	0.61	0.85		0.93	0.98	1.17	2.85			
FeO	9.80	0.55	8.03	0.44	0.50	0.44	1.03		2.09	0.67	2.14		1.68	1.74	2.68	11.08			
MnO	0.18	0.01	0.15	0.01	0.01	0.01	0.01		0.03	0.02	0.05		0.03	0.04	0.05	0.21			
MgO	4.52	0.53	4.44	0.32	0.37	0.43	0.22		1.36	0.42	1.89		1.20	1.76	1.84	5.79			
CaO	10.74	12.42	10.63	12.34	12.38	11.80	12.60		11.66	13.47	10.37		12.08	12.23	11.82	10.41			
Na_2O	2.60	3.65	2.72	3.68	3.68	4.19	3.53		3.77	3.09	4.02		3.60	3.51	3.49	2.04			
K_2O	1.04	0.84	1.18	0.71	0.73	0.95	0.60		0.68	0.46	0.72		0.56	0.55	0.72	0.43			
P_2O_5	2.32	0.04	1.25	0.09	0.07	0.07	0.24		0.13	0.07	0.09		0.20	0.14	0.30	0.22			
Total	98.36	97.98	95.61	97.41	97.66	97.01	95.45		96.40	96.70	94.62		96.15	96.35	96.49	93.99			
FeO^{total}	12.90	0.80	10.46	0.78	0.85	0.92	1.14		3.01	1.22	2.90		2.52	2.63	3.74	13.65			
Mg#[c]	38.5	54.1	43.1	42.2	43.9	45.5	25.6		44.5	38.1	53.7		45.9	54.4	46.7	43.1			
ppm																			
Rb	13.2	4.0	13.6	5.7	4.5	11.3	1.3	12.7	6.1	5.0	11.8	6.4	4.9	4.7	6.4	11.3	31	112	5.3
Ba	947	604	829	423	480	817	381	764	544	381	489	898	420	429	532	128	350	550	150
Th	0.7		0.8			2.5		4.4	1.9	0.5		0.6	1.3	0.7	1.1	2.0	4	10.7	1.1
Nb	14.3		12.0	1.5	2.9	1.7		10.3	6.9	2.2	3.6	3.9	1.7	3.4	5.8	9.6	48	25	6
La	21.5	7.5	14.8	5.8	6.8	5.8	8.0	12.3	7.5	8.5	5.8	9.7	7.4	8.1	9.1	11.8	37	30	11
Ce	40.8	3.1	27.1	5.7	4.3	4.3	12.7	26.0	12.4	6.2	4.0	5.1		11.6	14.2	24.0	80	64	23
Sr	665	996	658	925	950	908	916	678	974	1487	1246	1214	1106	1158	995	146	660	350	230
Nd			14.2	1.6	2.4		6.8	9.0	5.2	4.1		1.0		4.9	5.9	15.1	38.5	26	12.7
Zr	79.0	5.3	65.8	19.8	15.1	12.0	5.9	51.8	25.2	9.8	15.8	47.1	11.8	21.8	28.2	103.7	280	190	70
Y	22.8	2.0	17.3	4.7	3.3	1.5	2.7	12.4	5.6	3.3	2.3	5.2	2.4	4.4	6.5	32.3	29	22	19
Sc	34.8	10.1	28.2	13.8	10.6	9.8	12.0	31.9	16.2	15.1	5.6	6.9	13.9	13.2	16.9	47.9			14.9
V	304.7	6.7	222.4	13.8	14.6	18.5	7.8	148.5	74.8	1.5	49.0	27.3	39.1	46.0	76.3	333.7			
Cr	4.3		18.3				5.6		4.5		8.9	15.0	25.9	15.3	13.1	123.2			
Co	47.7	3.4	40.8	3.0	4.3	5.6	6.8	27.8	12.7	3.2	11.1	6.3	9.9	10.2	16.4	58.3			104
Ni	6.0		11.7	0.3	0.2	0.1		1.6	8.1		4.4	0.5	5.0	6.1	7.1	57.8			2080
Cu	42.3		24.8					21.7	10.0				17.4	9.4	13.5	80.5			28
Zn	108.6	0.9	87.9	6.8	4.7	8.0	3.1	75.3	23.4	4.4	19.2	19.5	10.0	14.1	26.4	101.5			
Ga	24.3	22.9	24.1	25.2	24.2	23.9	24.5	24.5	25.0	25.9	23.8	27.5	23.2	24.6	24.6	18.7			
ppm ratio																			
Zr/Y	3.46	2.65	3.81	4.21	4.58	8.00	2.19	4.18	4.47	2.97	6.87	9.06	4.92	4.97	4.35	3.21	9.66	8.64	3.68
Nb/Y	0.63		0.69	0.32	0.86	1.13		0.83	1.22	0.67	1.57	0.75	0.71	0.78	0.89	0.30	1.66	1.14	0.32
Zr/Nb	5.52		5.49	13.20	5.30	7.06		5.03	3.65	4.45	4.39	12.08	6.94	6.38	4.87	10.76	5.83	7.60	11.67
La/Nb	1.50		1.24	3.87	2.40	3.41		1.19	1.08	3.86	1.61	2.49	4.35	2.37	1.56	1.22	0.77	1.20	1.83
La/Nd			1.05	3.63	2.85		1.18	1.37	1.42	2.07		9.70		1.65	1.55	0.78	0.96	1.15	0.87
Th/Ce	0.02		0.03			0.58		0.17	0.16	0.08		0.12		0.06	0.08	0.08	0.05	0.17	0.05

All concentrations except FeO determined by wavelength dispersive X-ray fluorescence spectrometry; FeO determined by wet chemistry;[a] avg: Average with number of analyses in parentheses (includes data from Mukherjee et al. 2005); BenAn: Bengal anorthosite; Lti-meta: Low-Ti metabasic (Ghose et al. 2005); OIB: Ocean Island Basalt (Sun and McDonough, 1989); UCC and LCC: Upper and Lower Continental Crust (Taylor and McLennan, 1995); [b] 1 - NNE of Ledapalash; 2 - Nimra; 3 - Nandanpur; 4 - NW of Nandanpur; 5 - 13 km WNW of Gangajalghati; 6 - W of Shyampur; [c] Mg# = 100[Mg/(Mg+Fe)]

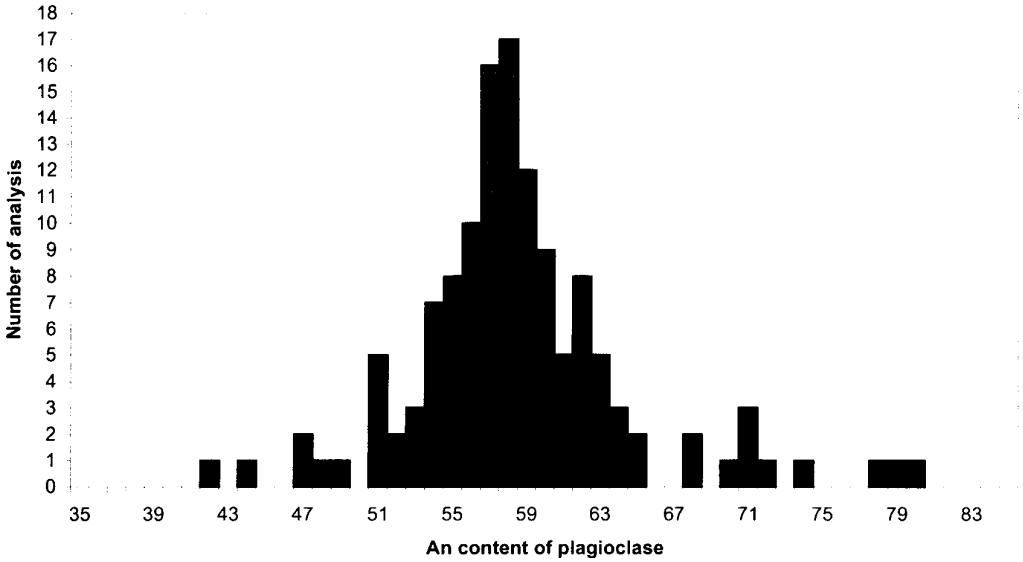

Fig.4. A frequency distribution of the anorthite-content of plagioclase in the Bengal anorthosite based on 136 analyses from six anorthosite samples, performed with the electron microprobe. The data show a well constrained peak around An_{57}.

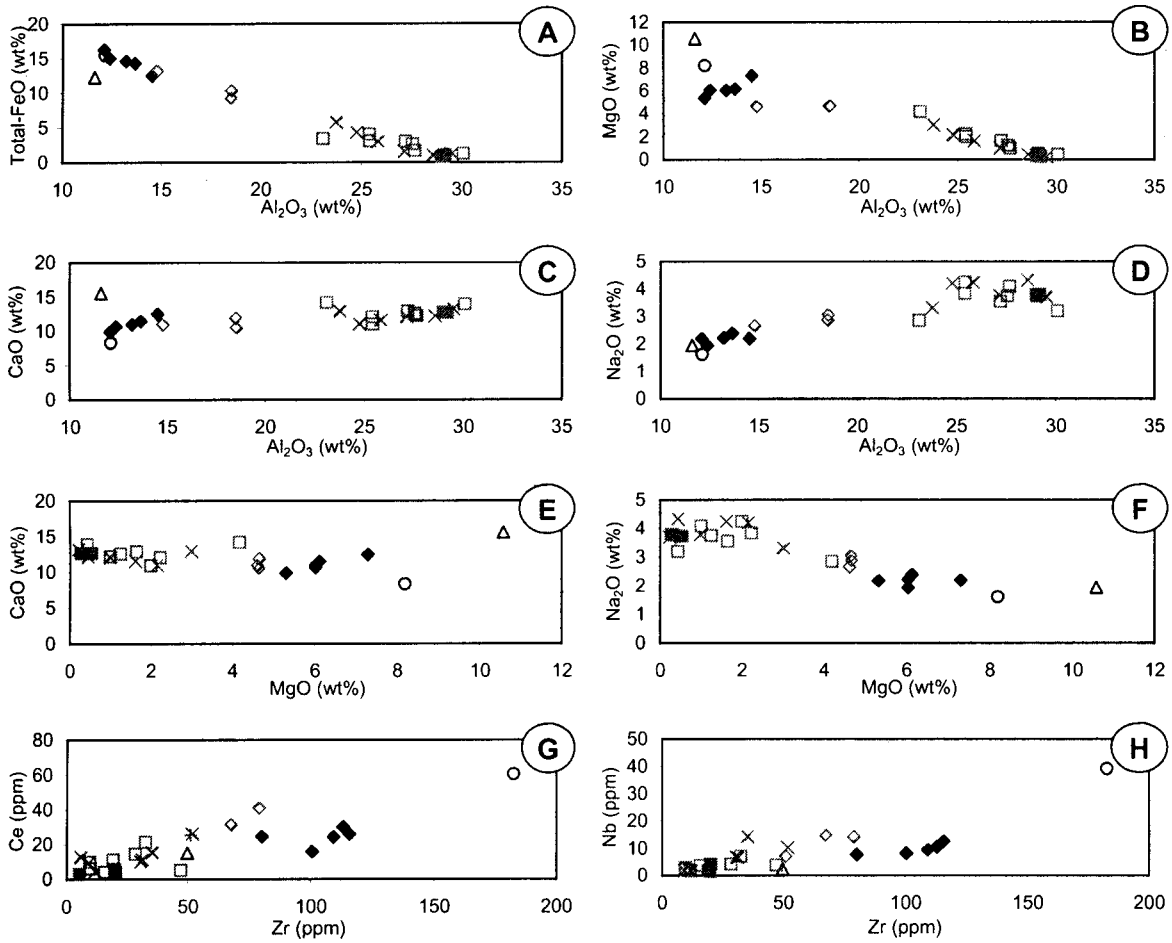

Fig.5. Variation of (A-D) Al_2O_3 and (E,F) MgO with total-FeO, CaO and Na_2O, and (G,H) Zr with Ce and Nb. Symbols: open square-white anorthosite; solid square-grey anorthosite; cross- mottled anorthosite; open diamond-gabbroic anorthosite; solid diamond: Low-Ti metabasic intrusive; circle: High-Ti metabasic intrusive; triangle: ultramafic intrusive.

Table 5. Rare-earth and high-field-strength element concentrations of selected Bengal anorthosite samples

	35SL White	26SL Mottled	27SL Gabbroic	33SL Gabbroic	Average
			parts per million[a]		
Sc	7.1	2.2	39	8.7	14.3
Th	0.6	0.1	0.7	0.3	0.4
Ta	0.65	0.17	1.4	0.15	0.59
Hf	0.9	0.37	2.5	0.54	1.08
La	5.6	7.8	13	12	9.6
Ce	20	10	20	18	17.0
Sm	1.92	0.53	2.87	1.74	1.77
Eu	1.7	1.9	1.8	2.4	2.0
Tb	0.13	0.05	0.22	0.14	0.14
Yb	0.12	0.17	0.59	0.39	0.32
Lu	0.12	0.03	0.2	0.03	0.10

[a] All concentrations determined by Neutron Activation Analysis

compared to white anorthosite. However, all the varieties of anorthosite plot on the same trends in inter-element variation diagrams indicating their common origin (Fig. 5). MgO and FeO are negatively correlated, and CaO and Na_2O are positively correlated with Al_2O_3 (Figs. 5A-D). Na_2O is positively correlated, whereas, CaO does not vary significantly with MgO (Figs. 5E-F). Nb and Ce are positively correlated with Zr (Figs. 5G-H). The average trace element pattern of the Bengal anorthosite is similar to that of the Bolangir anorthosite of the Eastern Ghats (Bhattacharya et al. 1998) but the contents are higher in the Bengal anorthosite. Both the Bengal and the Bolangir anorthosites show high positive Sr and Eu anomalies reflecting their feldspar cumulate nature.

Similar average Zr/Nb, Zr/Hf and Th/Ce ratios of the Bengal anorthosite and oceanic island basalt (Table 4, Hf from Table 5, Zr/Hf=34.6) possibly indicates derivation of the anorthosites from a mantle source. Prolonged interaction of the parental melts with the lower crust may be the reason for similar average Zr/Y, La/Nb and Th/Ce ratios of the anorthosites and lower continental crust (Table 4), whereas, interaction with the upper crust may have resulted in an enriched LILE pattern of the anorthosite (Fig. 6). Upper crustal anatexis may have happened through heat from the anorthositic magma. Anatectic leptynite and alkali granite with trace element patterns similar to that of a partial melt of typical upper crustal garnet-biotite country gneiss are present in the vicinity of the anorthosite (Ghose and Chatterjee, 2007). Upper crustal contamination is also indicated by similar trace element patterns of the anorthosites and syenite and high-Ti metabasic sample from a borehole in the anorthosite (Ghose et al. 2005; Ghose and Chatterjee, 2007).

The associated metabasic rocks are Fe- and LILE-rich tholeiites that can be related by fractional crystallization of olivine, augite and plagioclase (Ghose et al. 2005). In inter-element variation diagrams, the metabasic rocks plot on the same trends as the anorthosites (Fig.5), suggesting that the two groups may be genetically related. However, the average Zr/Nb and La/Nd ratios of the two groups are different (Table 4). The metabasic rocks have a lower crustal signature as indicated by a similarity of their average Zr/Y, Nb/Y and Zr/Nb ratios to the corresponding ratios of the lower continental crust (Table 4). The gabbroic anorthosites have Zr/Nb, La/Nd, Zr/Y, Nb/Y and La/Nb ratios intermediate between the metabasic rocks and the grey/mottled/white anorthosites (Table 4) indicating that they may have

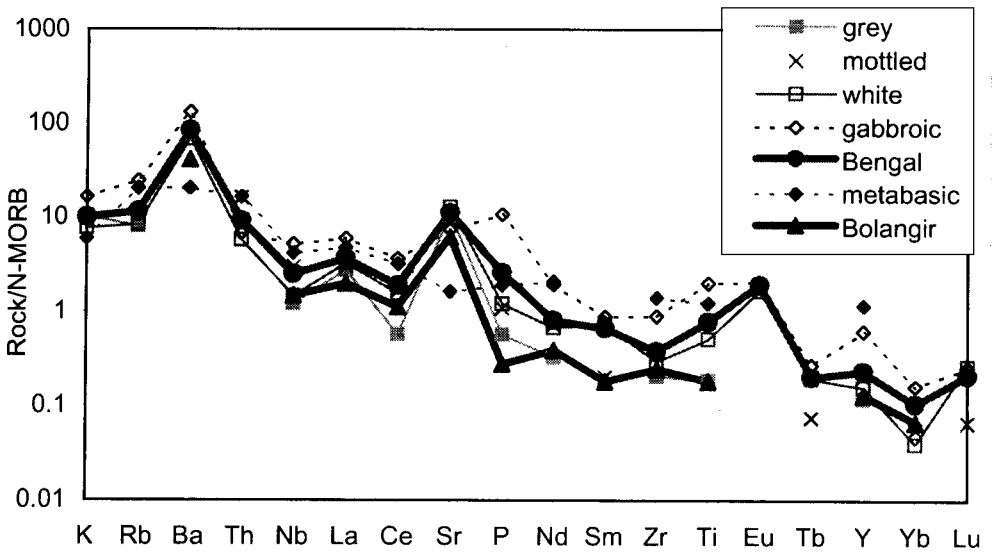

Fig.6. N-MORB-normalized (Sun and McDonough, 1989) incompatible element contents of the Bengal anorthosites (average of this study and Mukherjee et al. 2005) compared with the Bolangir anorthosite of Eastern Ghats (Bhattacharya et al.1998).

originated through mixing between anorthositic and precursor of metabasic end-members. Their high-Fe and high-incompatible element contents probably indicate that they are differentiated products of a parental mafic magma.

DISCUSSION

Igneous textures preserved in the Bengal anorthosite include magmatic flow related alignment of cumulus plagioclase in the core of the massif and alignment of euhedral plagioclase in anorthosite dykes. Zircon cores with magmatic oscillatory and sector zoning yielded a concordant U-Pb crystallization age of 1550 ± 2 Ma of the anorthosite (Chatterjee et al.2007). These original textures have been overprinted by cooling, hydration with H_2O released from surrounding crust, and subsequent poly-metamorphism that first stabilized hornblende and then augite, orthopyroxene and coronal garnet and zircon overgrowth rims by dehydration with progressive heating and loading at 0.9-1 Ga (Chatterjee et al. 2007; Maji et al. 2007). The silicate minerals equilibrated with the changing P-T conditions and their compositions (Table 3) reflect the conditions (Table 2, Fig. 3) of post-D_3 Grenvillian metamorphism (Maji et al. 2007).

The depth-profiles from a borehole in the anorthosite show cyclic variations in lithology, major and trace element contents, and elemental ratios indicating magma emplacement in pulses (Mukherjee et al. 2005). Also observed are chemical variations within each cycle, which may be explained by flotation of the grey plagioclase megacrysts over the anorthite-rich and relatively heavier white granular plagioclase. Higher concentrations of transitional major and trace elements in the white anorthosite have been related to sinking of Fe-Ti oxides. These geochemical and lithological characteristics are consistent with an igneous origin of the Bengal anorthosite. The geochemical features of the Bengal anorthosite also indicate a mantle origin, interaction and mixing with the lower crustal tholeiitic melts, and contamination with upper crustal anatectic melts.

Several tectono-thermal events in the central and eastern Indian shield have been recognized from different sectors of the Central Indian Tectonic Zone (CITZ, e.g. Sausar Mobile Belt, 2.1 Ga and 1.7-1.5 Ga, Acharyya, 2003; Bhowmik et al. 2005), the Singhbhum Mobile Belt (1.68-1.6 Ga, Sarkar et al. 1989; Sengupta et al.1994; Roy et al. 2002), and in the Eastern Ghats Belt (EGB, 1.6 Ga, Mezger and Cosca, 1999; Shaw et al. 1997). These events may be related to globally recognized episodes of granulite facies metamorphism, mantle-upwelling, crustal melting and granite intrusion (Peucat et al.1999; Oliver and Fanning, 1997). Deformation and high-grade metamorphism in the CGC during the Paleo- to Mesoproterozoic transition has been advocated by earlier workers (Pandey et al.1986; Mallik et al.1991; Ray Barman et al.1994) and interpreted as related to collision between the northern and southern Indian blocks both in the CGC (Sarkar, 1988) and in the CITZ (Yedekar et al.1990; Jain et al.1991; Mishra et al. 2000). The emplacement of the Bengal anorthosite postdating the early ca. 1.7-1.6 Ga tectono-thermal event in the CGC by ca. 50-150 Myr is consistent with a period of quiescence between delamination of lower lithosphere during compactional orogenesis and post-tectonic anorthosite emplacement required for the neutralization of horizontal forces through plateau uplift (McLelland et al. 2004).

Structural study has shown that the Damodar Graben formed after the formation of the penetrative fabric of the terrain (Sarkar, 1988). However, it is not clear if the graben is post-D_1/pre-D_2 or post-D_2. If the graben is pre-D_2, there is a possibility that it is related to the emplacement of the Bengal anorthosite. In such a case, the Bengal anorthosite may have originated in an extensional setting.

Acknowledgements: Borehole samples were obtained from a deep drilling project in the Bengal anorthosite undertaken by the Geological Survey of India with DM as in-charge. The neutron-activation REE analysis was carried out at the Geochemical Laboratory, Pune, India. Major and trace elements of rocks were analyzed by N. G. Marsh, at the Department of Geology, Leicester University. FeO was analyzed by Anjali Gupta at the Department of Geology, Patna University.

References

ACHARYYA, S.K. (2003) The nature of Mesoproterozoic central Indian tectonic zone with exhumed and reworked older granulites. Gondwana Res., v.6/2, pp.197-214.

ANDERSON, J.L. and SMITH, D.R. (1995) The effect of temperature and fo_2 on the Al-in-hornblende barometer. Amer. Mineral., v.80, pp.549-559.

ARMSTRONG, J.T. (1995) CITZAF - A package for correction programs for the quantitative electron microbeam X-ray analysis of thick polished materials, thin-films and particles. Microbeam Analysis, v.4, pp.177-200.

ASHWAL, L.D. (1993) "Anorthosites". Springer-Verlag, Berlin, 421p.

BAKSI, A.K. (1995) Petrogenesis and timing of volcanism in the Rajmahal flood basalt province, northeastern India. Chem. Geol., v.121, pp.73-90.

BHATTACHARYA, A., RAITH, A., HOERNES,S. and BANERJEE, D. (1998) Geochemical evolution of the massif type anorthosite complex at Bolangir in the Eastern Ghats Belts of India. Jour. Petrol., v.39, pp.1169-1195.

BHATTACHARYYA, P.K. and MUKHERJEE, S. (1987) Granulites in and around the Bengal anorthosite, eastern India: genesis of coronal garnet and evolution of the granulite-anorthosite complex. Geol. Mag., v.124, pp.21-32.

BHOWMIK, S.K., BASU SARBADHIKARI, A., SPIERING, B. and RAITH, M. (2005) Mesoproterozoic reworking of Palaeoproterozoic ultrahigh-temperature granulites in the Central Indian Tectonic Zone and its implications. Jour. Petrol., v.46, pp.1085-1119.

BOSE, M.K. and ROY, A.K. (1966) Co-existing iron titanium oxide minerals in norites associated with anorthosites of Bengal, India. Econ. Geol., v.61, pp.555-562.

CHATTERJEE, N., CROWLEY, J.L. and GHOSE, N.C. (2007) Geochronology of the 1.55 Ga Bengal anorthosite and Grenvillian metamorphism in the Chotanagpur gneissic complex, eastern India. Precambrian Res., doi:10.1016/ j.precamres.2007.09.005

CHATTERJEE, S.C. (1959) The problem of anorthosites with special reference to the anorthosites of Bengal. Presidential Address, 46 Indian Sci. Cong. Proc., Sec. 2, pp.75-95.

DAS, A. and BHATTACHARYYA, C. (1999) Amphibolites from Tulin-Jhalida area, Puruliya District, West Bengal. Indian Jour. Geol., v.71, nos. 1 and 2, pp.143-161.

ELLIS, D.J. and GREEN, D.H. (1979) An experimental study of the effect of Ca upon garnet-clinopyroxene Fe-Mg exchange equilibria. Contrib. Mineral. Petrol., v.71, pp.13-22.

EMSLIE, R.F. (1978) Anorthosite massifs, rapakivi granites, and late Proterozoic rifting of North America. Precambrian Res., v.7, pp.61-98.

EMSLIE, R.F. (1985) Proterozoic anorthosite massifs. *In:* A. Toby and J.L.R. Touret (Eds.), The deep Proterozoic crust in the North Atlantic provinces. NATO ASI Ser C, 158, Reidel, Dordrecht, pp.39-60.

EMSLIE, R.F., HAMILTON, M.A. and THERIAULT, R.J. (1994) Proterozoic anorthosite- mangerite- charnockite- granite (AMCG) complex; isotopic and chemical evidence from the Nain Plutonic Suite. Jour. Geol., v.102/5, pp.539-558.

FERRY, J.M. and SPEAR, F.S. (1978) Experimental calibration of the partitioning of Fe and Mg between biotite and garnet. Contrib. Mineral. Petrol., v.66, pp.113-117.

GHOSE, N.C. (1983) Geology, tectonics and evolution of the Chhotanagpur granite gneiss complex, Eastern India. *In:* S. Sinha-Roy (ed.), Structure and Tectonics of Precambrian Rocks of India, Recent Researches in Geology 10, Hindustan Publishing Corp., pp.211-247, Delhi.

GHOSE, N.C. (1992) Chhotanagpur gneiss-granulite complex Eastern India: Present status and future prospect. Indian Jour. Geol., v.84, pp.100-121.

GHOSE, N.C. and CHATTERJEE, N. (2007) Petrology, tectonic setting and source of dykes and related magmatic bodies in the Chotanagpur Gniessic Complex, Eastern India. *In:* R.K. Srivastava, Ch. Sivaji and N.V. Chalapathi Rao, (Eds.), Indian Dykes. Narosa Publ. House, New Delhi, in press.

GHOSE, N.C. and MUKHERJEE, D. (2000) Chhotanagpur gneiss-granulite complex, Eastern India – A kaleidoscope of global events. *In:* A. N. Trivedi, B.C. Sarkar, N.C. Ghose and Y.R. Dhar (eds.), Geology and Mineral Resources of Bihar and Jharkhand, Platinum Jubilee Commemoration Volume, Indian School of Mines, Dhanbad, Institute of Geoexploration and Environment Mono., v.2, pp.33-58, Patna.

GHOSE, N.C., SHMAKIN, B.M. and SMIRNOV, V.N. (1973) Some geochronological observations on the Precambrians of Chhotanagpur, Bihar. Geol. Mag., v.110, pp.481-484.

GHOSE, N.C., MUKHERJEE, D. and CHATTERJEE, N. (2005) Plume generated Mesoproterozoic mafic-ultramafic magmatism in the Chotanagpur mobile belt of Eastern Indian shield margin. Jour. Geol. Soc. India, v.66, pp.725-740.

GOVINDARAJU, K. (1994). 1994 compilation of working values and sample description for 383 geostandards. Geostandards Newsletter, Special Issue, v.18, pp.1-158.

GRAHAM, C.M. and POWELL, R. (1984) A garnet-hornblende geothermometer: calibration, testing and application to the Pelona Schist, Southern California. Jour. Metamorphic Geol., v.2, pp.13-21.

GREEN, T.H. (1969) High-pressure experimental studies on the origin of anorthosite. Canadian Jour. Earth Sciences, v.6, pp.427-440.

GROVE, T.L. (1977) Structural characterization of labradorite-bytownite plagioclase from volcanic, plutonic and metamorphic environments. Contrib. Mineral. Petrol., v.64, pp.273-302.

HOLLAND, T. and BLUNDY, J. (1994) Non-ideal interactions in calcic amphiboles and their bearing on amphibole-plagioclase thermometry. Contrib. Mineral. Petrol., v.116, pp.433-437.

JAIN, S.C., YEDEKAR, D.B. and NAIR, K.K.K. (1991) Central Indian shear zone: a major Precambrian crustal boundary. Jour. Geol. Soc. India, v.37, pp.521-531.

KENT, R.W., PRINGLE, M.S., MULLER, R.D., SAUNDERS, A.D. and GHOSE, N.C. (2002) $^{40}Ar/^{39}Ar$ geochronology of the Rajmahal basalts, India and their relationship to the Kerguelen Plateau. Jour. Petrol., v.43, pp.1141-1153.

LINDSLEY, D.H. (1983) Pyroxene thermometry. Amer. Mineral., v.68, pp.477-493.

LONGHI, J.(2005) A mafic or mantle crustal source for Proterozoic anorthosites? Lithos, v.8, pp.183-198.

LONGHI, J., VANDER AUWERA, J., FRAM, M.S. and DUCHESNE, J-C. (1999) Some phase equilibrium constraints on the origin of Proterozoic (Massif) Anorthosites and related rocks. Jour. Petrol., v.40, pp.339-362.

MAJI, A.K., GOON, S., BHATTACHARYA, A., MISHRA, B., MAHATO, S. and BERNHARDT, H.-J. (2007) Proterozoic polyphase metamorphism in the Chhotanagpur Gneissic Complex (India), and implication for trans-continental Gondwanaland

correlation. Precambrian Res., doi:10.1016/j.precamres.2007.10.002

MALLIK, A.K., GUPTA, S.N. and RAY BARMAN, T. (1991) Dating of early Precambrian granite-greenstone complex of the Eastern Indian Precambrian shield with special reference to the Chotanagpur granite gneiss complex. Rec. Geol. Surv. India, v.125, pt. 2, pp.20-21.

MANNA, S.S. and SEN, S.K. (1974) Origin of garnet in the basic granulites around Saltora, W. Bengal, India. Contrib. Mineral. Petrol., v44, pp.195-218.

MCLELLAND, J.M., BICKFORD, M.E., HILL, B.M., CLECHENKO, C.C., VALLEY, J.W. and HAMILTON, M.A. (2004) Direct dating of Adirondack massif anorthosite by U-Pb SHRIMP analysis of igneous zircon: implications for AMCG complexes. Geol. Soc. Amer. Bull., v.116, pp.1299-1317.

MEZGER, K. and COSCA, M.A. (1999) The thermal history of the Eastern Ghats (India) as revealed by U-Pb and $^{40}Ar/^{39}Ar$ dating of metamorphic and magmatic minerals: implications for the SWEAT correlation. Precambrian Res., v.94, pp.251-271.

MISHRA, D.C., SINGH, B., TIWARI, V.M., GUPTA, S.B. and RAO, M.B.S.V. (2000) Two cases of continental collisions and related tectonics during the Proterozoic period in India: insights from gravity modelling constrained by seismic and magnetotelluric studies. Precamb. Res., v.99, pp.149-169.

MUKHERJEE, D. (1995) Geochemical and tectonic evolution of Bengal anorthosite. Unpub. Ph. D. Thesis, Patna University, Patna.

MUKHERJEE, D. and GHOSE, N.C. (1992) Precambrian anorthosites within the Chhotanagpur gneissic complex in Eastern Indian Shield. Indian Jour. Geol., v.64, pp.143-150.

MUKHERJEE, D., GHOSE, N.C. and CHATTERJEE, N. (2005) Crystallization history of a massif anorthosite in Eastern Indian shield margin based on borehole lithology. Jour. Asian Earth Sci., v.25, pp.77-94.

MUKHOPADHYAY, M. (1987) Gravity field and its significance to the origin of Bengal anorthosite. Jour. Geol. Soc. India, v.29, pp.489-499.

NEWTON, R.C. and PERKINS, D. III (1982) Thermodynamic calibration of geobarometers based on the assemblage garnet-plagioclase-orthopyroxene-(clinopyroxene)-quartz. Amer. Mineral., v.67, pp.203-222.

OLIVER, R.L.and FANNING, M. (1997) Antarctica: Precise correlation of Paleoproterozoic terrains. *In:* C.A. Ricci (Ed.), The Antarctica Region: geological evolution and processes. Terra Antarctica Publ., Siena, pp.163-172.

PANDEY, B. K., GUPTA, J. N. and LALL, Y. (1986) Whole rock and Rb-Sr isochron ages for the granites from Bihar mica belt of Hazaribagh, Bihar, India. Indian Jour. Earth Sci., v.12, pp.157-162.

PEUCAT, J.J., MENO, R.P., MONNIER, O. and FANNING, C.M. (1999) The Terra Adelie basement in the east Antarctica shield: Geological and isotopic evidence for a major 1.7 Ga thermal event; comparison with Gwalior craton in South Australia. Precambrian Res., v.94, pp.205-224.

RAY BARMAN, T. and BISHUI, P. K. (1994) Dating of Chotanagpur gneissic complex of eastern Indian Precambrian shield. Rec. Geol. Surv. India, v.127, pt.2, pp.23-24.

RAY BARMAN, T., BISHUI, P.K., MUKHOPADHYAY, K. and RAY, J.N. (1994) Rb-Sr geochronology of the high grade rocks from Purulia, West Bengal, and Jamua-Dumka sector, Bihar. Indian Minerals, v.48, pp.45-60.

ROY, A.K. (1977) Structural and metamorphic evolution of the Bengal Anorthosite and associated rocks. Jour. Geol. Soc. India, v.18, pp.203-223.

ROY, A., SARKAR, A., JEYKUMAR, S., AGGRAWAL, S.K. and EBIHARA, M. (2002) Mid-Proterozoic plume-related thermal event in Eastern Indian craton: Evidence from trace elements, REE geochemistry and Sr-Nd isotope systematics of basic-ultrabasic intrusives from Dalma volcanic belt. Gondwana Res., v.5, pp.133-146.

ROYSE, K.R. and PARK, R.G. (2000) Emplacement of the Nain anorthosite: diapiric versus conduit ascent. Canadian Jour. Earth Sci., v.37, pp.1195-1207.

SARKAR, A.N. (1988) Tectonic evolution of the Chotanagpur Plateau and the Gondwana Basins in Eastern India: an interpretation based on supra-subduction geological processes. *In:* D. Mukhopadhaya (Ed.), "Precambrian of the Eastern Indian Shield", Mem. Geol. Soc. India, no.8, pp.127-148.

SARKAR, A., BHANUMATI, L. and BALASUBRAHMANYAN, M.N. (1981) Petrology, geochemistry and geochronogy of the Chilka Lake igneous complex, Orissa state, India. Lithos, v.14, pp.93-111.

SARKAR, A., GUPTA, S.N., RAY BARMAN, T. and BISHUI, P.K. (1989) Dating of early Precambrian granite-greenstone complex of the eastern Indian Precambrian shield – special reference to Chotanagpur gneissic complex. Rec. Geol. Surv. India, v.122, pt. 2, pp.26-27.

SEN, S.K. and BHATTACHARYA, A. (1985) Fluid induced metamorphic changes in the Bengal anorthosite around Saltora, West Bengal, India. Indian Jour. Earth Sci., v.13, pp.45-64.

SEN, S.K. and BHATTACHARYA, A. (1993) Post peak pressure-temperature-fluid history of the granulites around Saltora, West Bengal. Proc. National Acad. Sci. India, v.63(A) 1, pp.280-306.

SEN, S.K. and MANNA, S.S. (1976) Patterns of cation fractionation among pyroxenes, hornblende and garnet in the basic granulites of Saltora, West Bengal. Indian Jour. Earth Sci., v.3, pp.117-128.

SENGUPTA, J.G., PAUL, D.K., BISHUI, P.K., GUPTA, S.N., CHAKRABORTY, R. and SEN, P. (1994) Geochemical and Rb-Sr isotopic study of Kuilapal granite and Arkasani granophyre from the eastern Indian craton. Indian Minerals, v.48, pp.77-88.

SHAW, R.K., ARIMA, M., KAGAMI, H., FANNING C.M., SHIRAISHI, K. and MOTOYOSHI, Y. (1997) Proterozoic events in the Eastern Ghats belt: evidence from Rb-Sr, Sm-Nd sytematics, and SHRIMP dating. Jour. Geol., v.105, pp.645-656.

SINGH, R.N., THORPE, R. and KRISTIC, D. (2001) Galena Pb isotope data of base metal occurrences in the Hesatu-Belbathan belt, eastern Precambrian shield, Bihar. Jour. Geol. Soc. India, v.57, pp.535-538.

SUN, S.S. and MCDONOUGH, W.F. (1989) Element concentrations (in ppm) for chondrites, normal enriched-type, mid-ocean ridge basalts (N- and E-MORB), and ocean island basalt (OIB). *In:* A.D. Saunders and A.J. Norry (Eds.), Magmatism in the Ocean Basins. Geol. Soc. Amer. Spec. Publ., no. 42, pp.313-345.

TAYLOR, S.R. and MCLENNEN, S.M. (1995) The geochemical evolution of the continental crust. Rev. Geophys., v.33, pp.241-265.

TAYLOR, S.R., CAMPBELL, I.H., MCCULLOCH, M.T. and MCLENNAN, S.M. (1984) A lower crustal origin of massif-type anorthosites. Nature, v.311, pp.372-374.

VERMA, R.K., GHOSE, D., ROY, S.K. and GHOSE, A. (1975) Gravity survey of Bankura anorthosite complex, West Bengal. Jour. Geol. Soc. India, v.16, pp.361-369.

WIEBE, R.A. (1994) Proterozoic anorthosite complexes. *In:* K.C. Condie (Ed.), "Proterozoic Crustal Evolution". Elsevier, Amsterdam, pp.215- 261.

YEDEKAR, D.B., JAIN, S.C., NAIR, K.K.K. and DUTTA, K.K. (1990) The Central Indian collisional zone. Geol. Surv. India, Special Publ., v.28, pp.1-28.

(Received: 25 June 2007; Revised form accepted: 31 January 2008)